Supporting information

Nitrogen Source-Regulated Biomass-Based COF@CNF Aerogel: Achieving Efficient Photothermal-Photocatalytic Synergy

Ranran Ji, Yaning Xu, Menglu Yang, Chengxu Zhou, Tiantian Wu, Yujie Zhao, Qing Huang, Dan Tian*

Co-Innovation Center of Efficient Processing and Utilization of Forest Resources, College of Materials Science and Engineering, Nanjing Forestry University, No. 159 Longpan Road, Nanjing 210037, PR China

**Corresponding author: E-mail: tiandan@njfu.edu.cn*

Experiment Section

Chemicals and Reagents

All solvents and reagents purchased from commercial sources are used directly without further purification.

1,3,5-Triformylphenol (TP, 98%), melamine (Tt, 98%), and melem (Ht, 98%) are purchased from Jilin Zhongkeyanshen Technology Co., Ltd. N, N-Dimethylformamide (DMF), N, N-Dimethylacetamide (DMA), dimethyl sulfoxide (DMSO), acetic acid (HAc), 3-Glycidyloxypropyltrimethoxysilane (GPTMS), tert-butanol (TBA), L-tryptophan (Trp), and p-benzoquinone (PBQ) are purchased from Aladdin Reagent Co., Ltd. (China). Tetrahydrofuran (THF, 99.5%) and 30% hydrogen peroxide stock solution are purchased from Sinopharm Chemical Reagent Co., Ltd. Polyethyleneimine (PEI) is purchased from Guangdong Wengjiang Chemical Reagent Co., Ltd. The CNFs suspension used in this study, with a solid content of 1.2 wt%, was purchased from Tianjin Wood Elf Biotechnology Co., Ltd., and the fiber size ranged from 20 to 40 μm.

Synthesis of TpTt and TpHt

The synthesis procedure of TpTt is described as follows [1]. A mixture of 0.3 mmol 1,3,5-triacetylphenol (Tp) and 0.3 mmol melamine (Tt) is added into a Pyrex tube, followed by the addition of a mixed solvent system consisting of 2 mL dimethyl sulfoxide (DMSO) and 1 mL N, N-dimethylacetamide (DMAc). Then, 0.3 mL of 6 M acetic acid (HAc) is introduced as a catalyst. The resulting mixture is ultrasonically dispersed and transferred into a sealed reaction vessel, followed by three freeze–pump–thaw cycles. The reaction is carried out at 120 °C for 72 h under solvothermal conditions. After completion, the system is naturally cooled to room temperature, and the obtained product is washed repeatedly with N, N-dimethylformamide (DMF) and tetrahydrofuran (THF). Subsequently, the sample is dried under vacuum at 80 °C for 12 h, yielding a brownish-yellow powder, denoted as TpTt.

The synthesis of TpHt is similar to that of TpTt, except that the amine monomer Tt is replaced by melem (Ht), while all other procedures remain unchanged [2]. Specifically, 0.3 mmol Tp and 0.3 mmol Ht are added into the reaction system and dissolved in 3 mL DMSO, followed by the addition of 0.3 mL 6 M HAc as a catalyst. After ultrasonic dispersion, the mixture undergoes three freeze-pump-thaw cycles and is then subjected to solvothermal reaction at 120 °C for 72 h. Upon completion, the product is washed thoroughly with DMF and THF. Finally, the sample is dried under vacuum at 80 °C for 12 h to obtain a brick-red powder, denoted as TpHt.

Preparation of COF@CNF aerogel and corresponding evaporator

First, mix GPTMS with CNF and stir for 0.5 hours. Then add PEI and continue stirring for 1 hour to obtain a uniform composite solution [3]. Subsequently, add TpTt or TpHt to the above system, mix thoroughly, and subject to ultrasonic treatment to achieve good dispersion and composite formation. For the non-directional freezing method, the mixture is poured into a cylindrical mold, pre-cooled in a -20 °C freezer to form a frozen block, and then freeze-dried for 2 days to obtain non-oriented COF@CNF with randomly distributed channels. For the oriented freezing method, the mixture is poured into a cylindrical mold placed on a pre-cooled copper plate, enabling unidirectional heat transfer from bottom to top. During freezing, ice crystals grow along the heat flow direction, guiding the ordered self-assembly of the CNF-COF network. The frozen block is subsequently freeze-dried for 2 days to yield oriented COF@CNF aerogel (TpTt@CNF and TpHt@CNF) with highly aligned, parallel channels. Finally, 2 mL of a carbon nanotube/isopropanol suspension with a concentration of 2.5 mg mL^{-1} was uniformly applied onto the aerogel surface via a drop-casting method. After each coating step, the sample was dried at 80 °C, and this process was repeated multiple times until a uniform coating layer was formed on the aerogel surface. Subsequently, the sample was vacuum-dried at 80 °C to obtain the oriented COF@CNF evaporator (TCE and HCE).

Characterization

The morphology and structure of the samples were investigated using scanning electron microscopy (SEM; FEI Quanta 200). Powder X-ray diffraction (PXRD) patterns were recorded on a Rigaku XRD Ultima IV diffractometer. X-ray photoelectron spectroscopy (XPS) spectra were acquired on a scanning X-ray microanalysis system (Shimadzu AXIS Ultra DLD). Fourier transform infrared (FT-IR) spectra were recorded using a Bruker VERTEX 80 V instrument. Mechanical property testing of the aerogels was performed on a SHIMADZU universal testing machine. Major ion concentrations were determined via inductively coupled plasma optical emission spectrometry (ICP-OES). Solution absorbance was analyzed using a UV spectrophotometer (UH5300).

Time-resolved photoluminescence (TRPL) spectra were performed on a FluoroMax Plus spectrofluorometer with an excitation wavelength of 400 nm and an emission wavelength of 470 nm. The fluorescence decay curves were fitted using a bi-exponential decay model:

$$I(t) = A_1 exp(-t/\tau_1) + A_2 exp(-t/\tau_2)$$

where τ_1 and τ_1 represent the fluorescence lifetime components, and A_1 and A_2 are the corresponding pre-exponential factors. The average fluorescence lifetime (τ_{avg}) was calculated using the amplitude-weighted formula:

$$\tau_{avg} = \frac{A_1\tau_1^2 + A_2\tau_2^2}{A_1\tau_1 + A_2\tau_2}$$

Differential scanning calorimetry (DSC) was conducted on a TA Instruments DSC250. Samples (~5-10 mg) were sealed in aluminum pans with a pinhole in the lid to ensure steady vapor escape. The measurements were carried out under a nitrogen atmosphere (flow rate: 50 mL/min) from 20 °C to 160 °C at a heating rate of 10 °C/min. The enthalpy of evaporation (ΔH_{vap}) was determined by integrating the endothermic peaks (70-120 °C) using TA Universal Analysis software.

Photoelectrochemical Measurements

Photoelectrochemical measurements are conducted on an electrochemical workstation (CS350M, CORRTEST, China) using a standard three-electrode electrochemical cell. The working electrode is a platinum plate, the counter electrode is a platinum plate, and the reference electrode is a saturated silver/silver chloride electrode. The electrolyte is a 0.2 M sodium sulfate solution.

Working electrode preparation: Mix 2 mg catalyst, 1 mL ethanol, and 10 μL Nafion D-520. Sonicate for 30 minutes. Then uniformly coat 200 μL of the slurry onto the surface of an ITO glass plate (1×2 cm^2). Allow to air dry.

Photothermal-Photocatalytic Performance experiments

Photothermal-photocatalytic performance experiments are conducted using a solar simulator equipped with an AM1.5G filter, capable of emitting simulated solar irradiance at 1000 W m^{-2} (1 sun). A circular sample approximately 25 mm thick with a top surface area of about 1.5 cm^2 is placed inside a glass bottle. The sample is embedded within hollow polystyrene (PS) foam floating on seawater. The sample is exposed to the simulator under stable solar radiation. Surface temperature changes were recorded using an infrared pyrometer, and evaporation rates are measured under steady-state conditions. Mass loss of the entire apparatus is recorded by an electronic mass balance. The water transmission rate (v) is calculated using the following equation:

$$v = \frac{Q}{2t_h}$$

Where t_h represents the water absorption (Q) from the dry state to the saturated state.

Hydrogen peroxide content is determined by iodometric titration. After photocatalytic treatment, 1 mL of potassium hydrogen phthalate ($C_8H_5KO_4$, 0.1 mol L^{-1}) aqueous solution and 1 mL of potassium iodide (KI, 0.4 mol L^{-1}) aqueous solution are added to 1 mL of seawater, which was then allowed to stand for 30 minutes. Under acidic conditions, hydrogen peroxide molecules react with iodide ions (I^-) to form iodide ions (I_3^-), which exhibit a strong absorption peak near 350 nm. The absorbance

of I_3^- at 350 nm is measured using a UV spectrophotometer (UH5300). The amount of H_2O_2 produced in each reaction is calculated based on the following chemical equation:

$$3I^- + H_2O_2 + 2H^+ \rightarrow I_3^- + 2H_2O$$

$$c(H_2O_2) = c(I_3^-)$$

Therefore, the concentration of H_2O_2 can be determined by measuring the I_3^- concentration.

The total solar energy conversion coefficient (SEC) of this system is calculated by summing the solar energy conversion values from the evaporation process and the catalytic preparation of H_2O_2.

$$SEC = SEC_{vapour} + SEC_{H_2O_2}$$

The solar energy conversion coefficient for the evaporation process (SEC_{vapour}) is calculated using the following formula:

$$SEC_{vapour} = m \times h_{Lv}$$

Where m is the steam generation rate (kg m^{-2} h^{-1}), and h_{Lv} is the latent heat of vaporization (≈2260 kJ kg^{-1}).

The calculation formula for $SEC_{H_2O_2}$ is as follows:

$$SEC_{H_2O_2} = r_{H_2O_2} \times \Delta G$$

where $r_{H_2O_2}$ is the H_2O_2 generation rate, and ΔG is the Gibbs free energy of the reaction (117 kJ mol^{-1}).

Table 1. Comparison of structural and electronic characteristics of COFs derived from different nitrogen sources (TpTt vs TpHt) [4-8].

Comparison Aspect	TpTt	TpHt
Building Unit	Triazine	Heptazine
Core Structure	Single triazine ring	Fused heptazine super-ring
π-conjugation extent	Relatively limited	More extended
Conjugation length	Shorter	Longer
Nitrogen site characteristics	Relatively localized	More abundant and distributed
Electronic structure feature	Higher electron localization	Enhanced electron delocalization

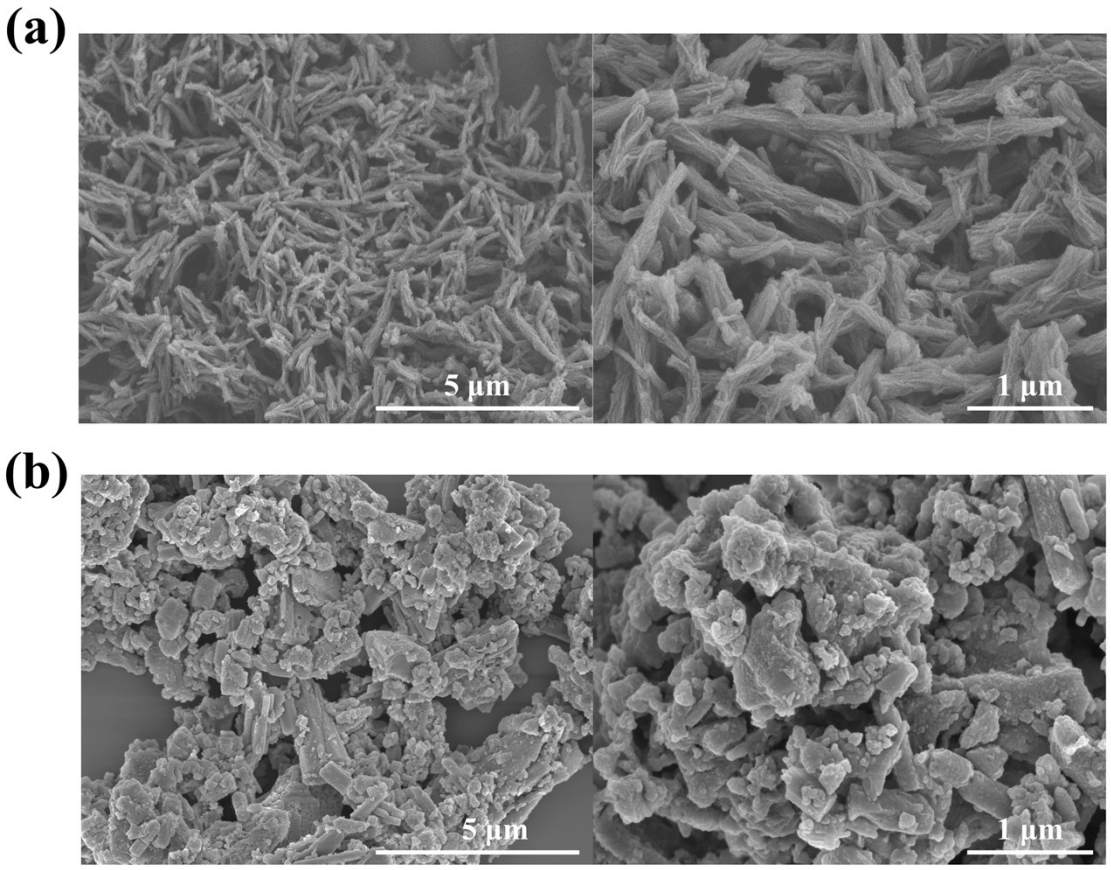

Figure S1. SEM images of (a) TpTt and (b) TpHt.

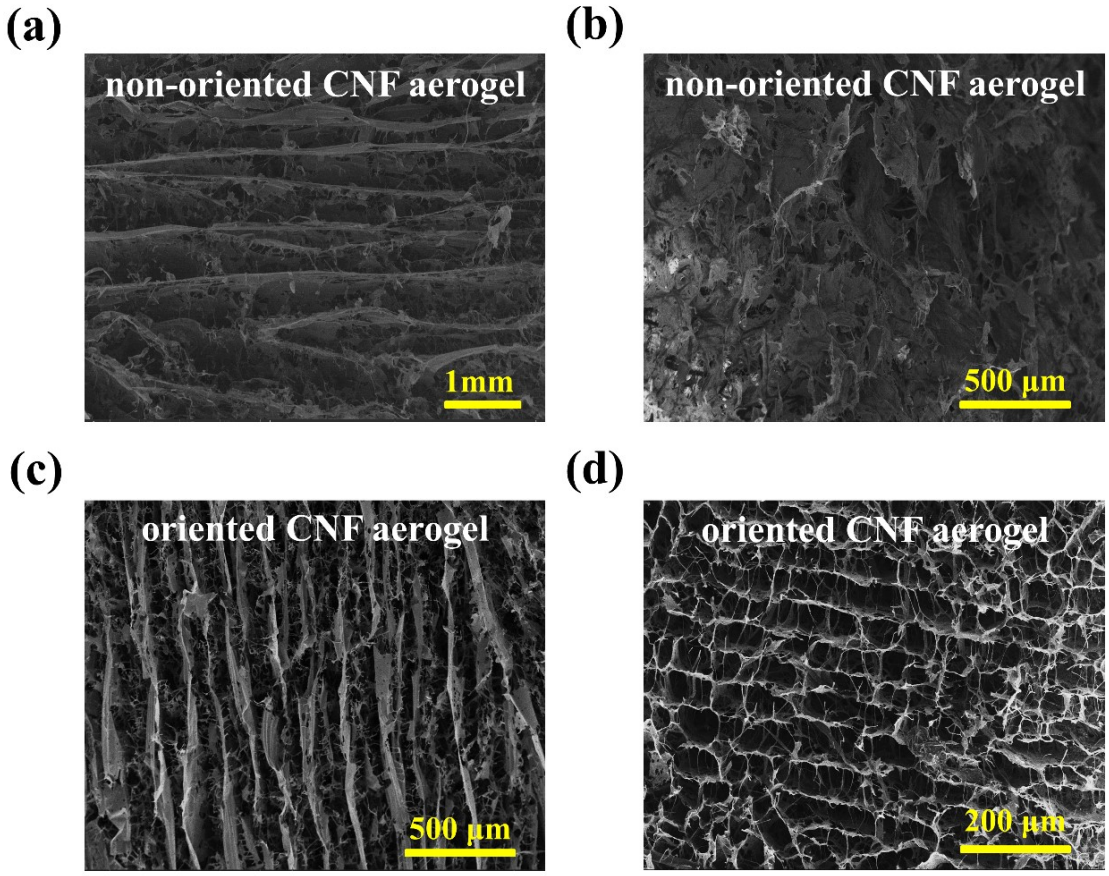

Figure S2. SEM image of non-oriented CNF aerogel (a) along the transverse direction; (b)along the longitudinal direction; SEM image of oriented CNF aerogel (c) along the transverse direction; (d) along the longitudinal direction.

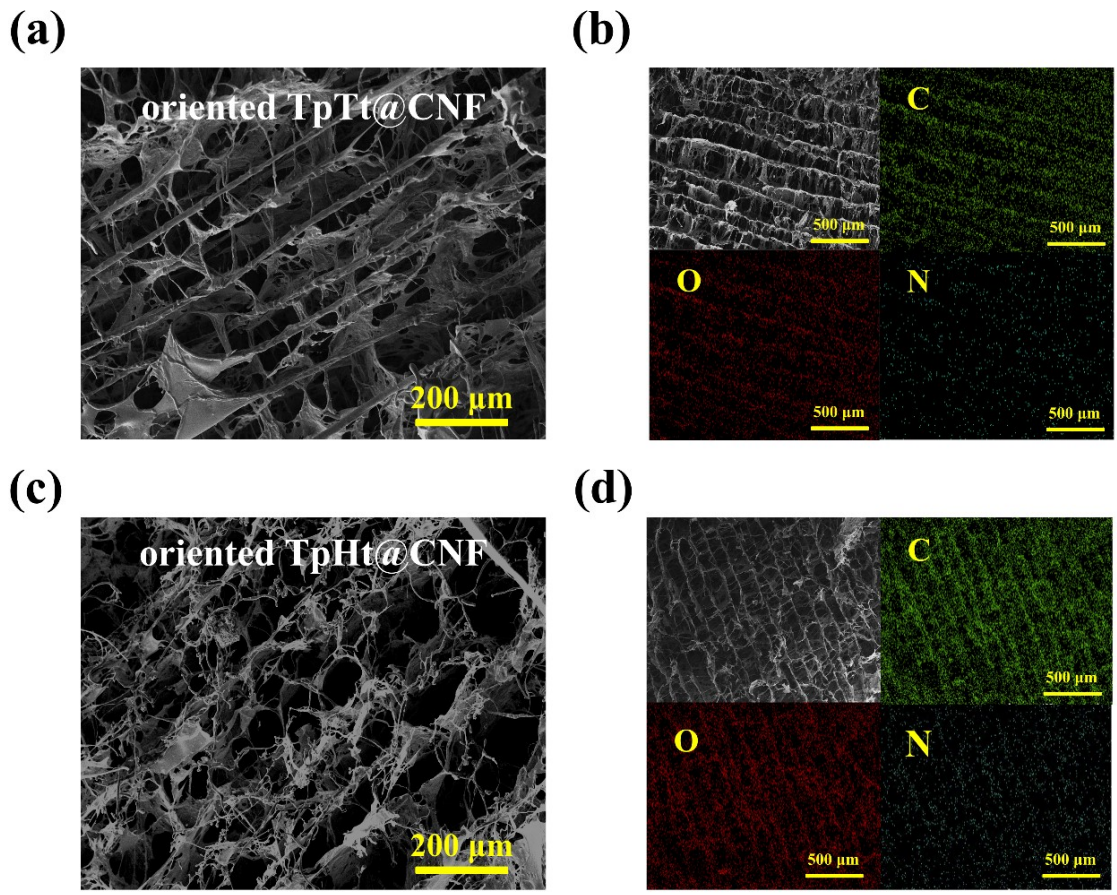

Figure S3. (a-b) SEM image (a) and EDS mapping image (b) of oriented TpTt@CNF along the transverse direction; (c-d) SEM image (c) and EDS mapping image (d) of oriented TpHt@CNF along the transverse direction;

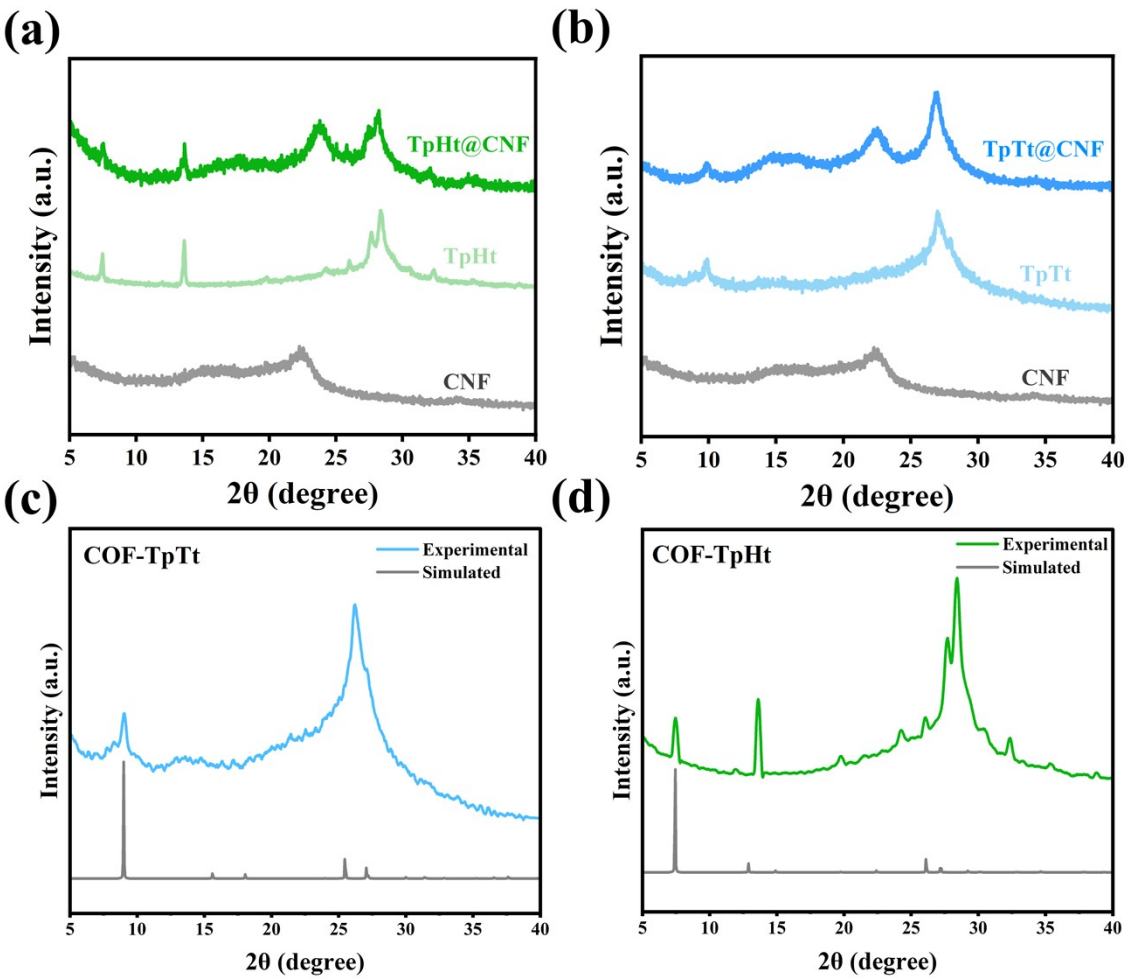

Figure S4. (a) PXRD patterns of CNF, TpTt, and TpTt@CNF aerogel; (b) PXRD patterns of CNF, TpHt, and TpHt@CNF aerogel. (c) Comparison between experimental and simulated PXRD patterns of TpTt; (d) Comparison between experimental and simulated PXRD patterns of TpHt.

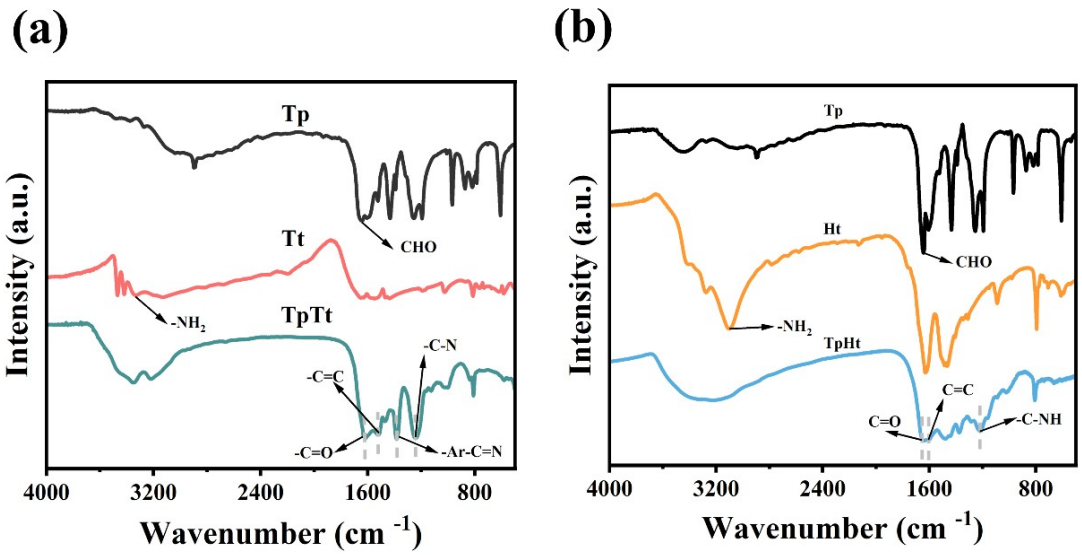

Figure S5. FTIR spectra of (a) TpTt, (b)TpHt, and their respective ligands.

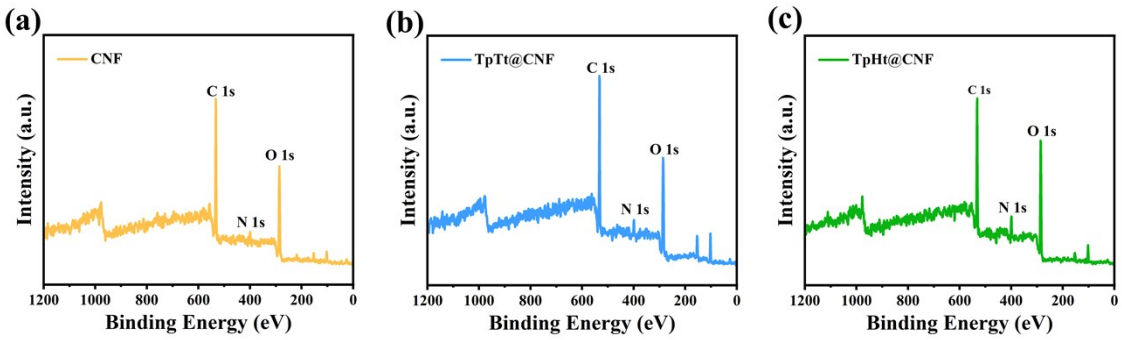

Figure S6. XPS spectra of (a) CNF, (b) TpTt@CNF, and (c) TpHt@CNF.

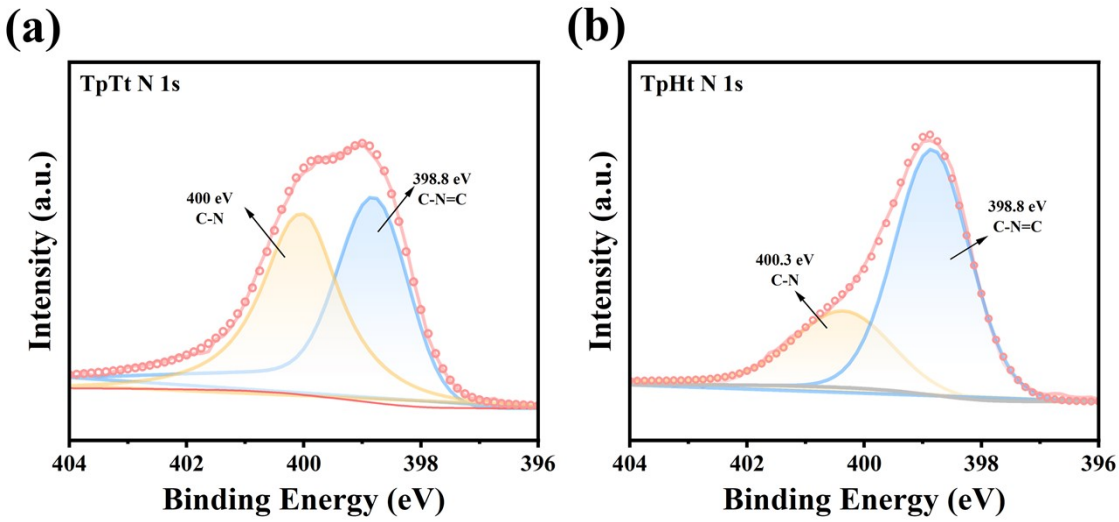

Figure S7. N1s XPS spectra of (a) TpTt and (b) TpHt.

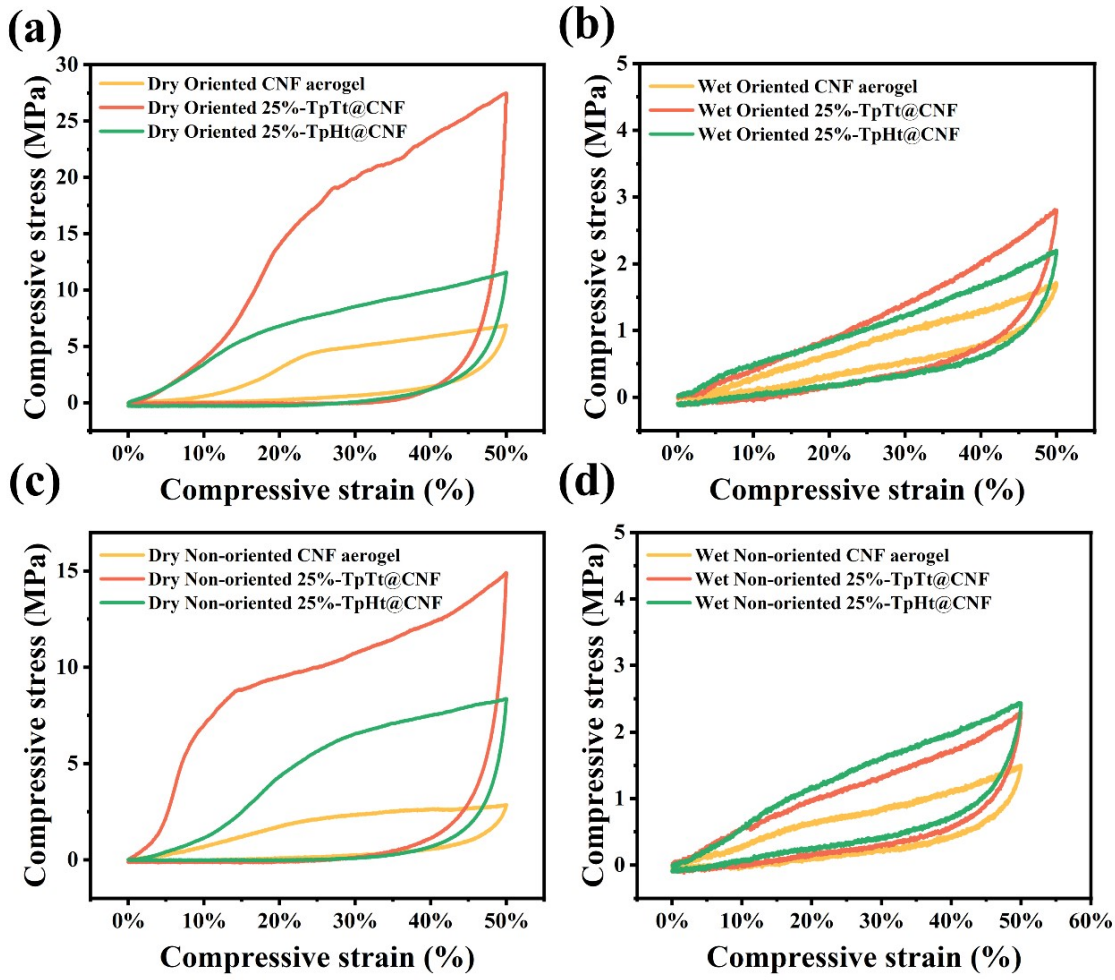

Figure S8. Mechanical response of oriented aerogel in **(a)** dry and **(b)** wet states under 50% strain. Mechanical response of non-oriented aerogel in **(c)** dry and **(d)** wet states under 50% strain.

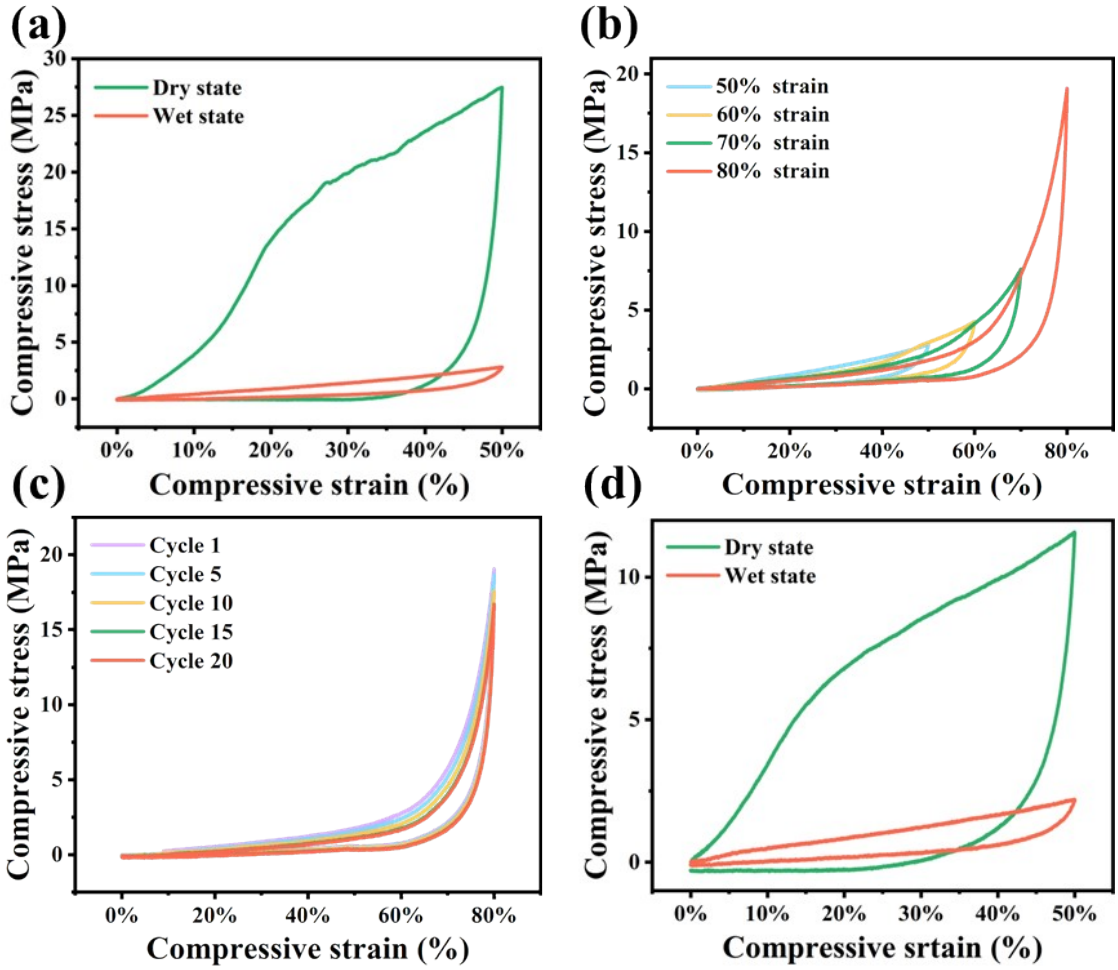

Figure S9. (a) Mechanical response of dry state and wet state oriented 25%-TpTt@CNF under 50% strain. (b) Stress-strain curves of wet oriented 25%-TpTt@CNF compressed to varying maximum strains. (c) Fatigue performance of wet oriented 25%-TpTt@CNF over 20 consecutive cycles at 80% strain. (d) Mechanical response of dry state and wet state oriented 25%-TpHt@CNF under 50% strain.

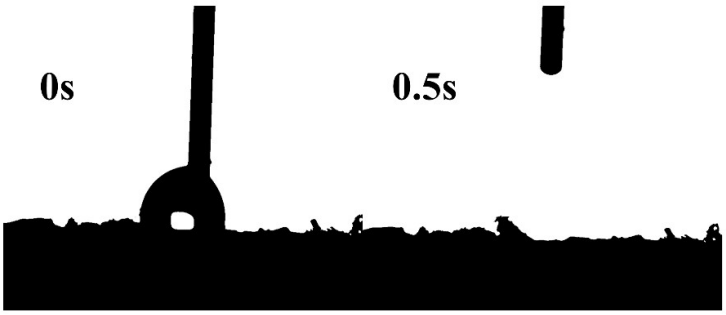

Figure S10. Surface static water contact angle of CNF aerogel.

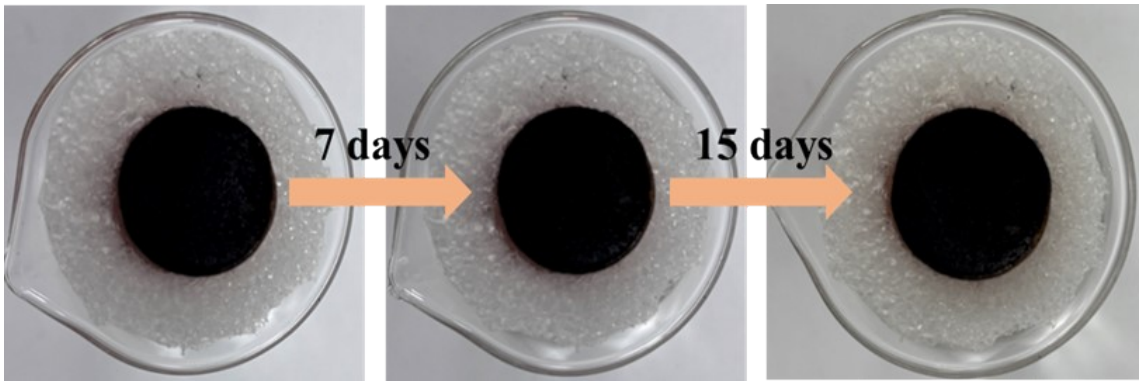

Figure S11. Structural stability of COF@CNF aerogel after 15 days of immersion in water.

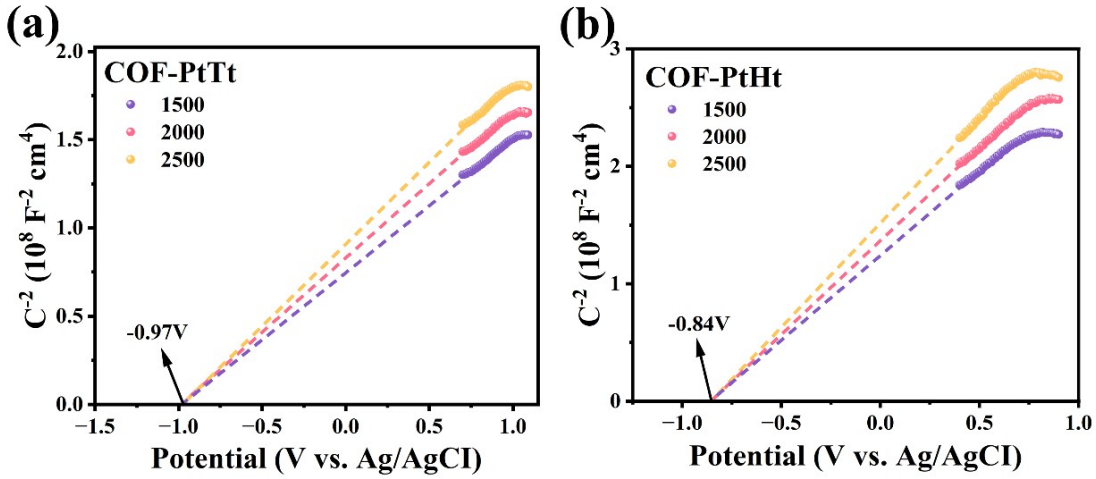

Figure S12. Mott-Schottky diagrams for (a) TpTt and (b) TpHt.

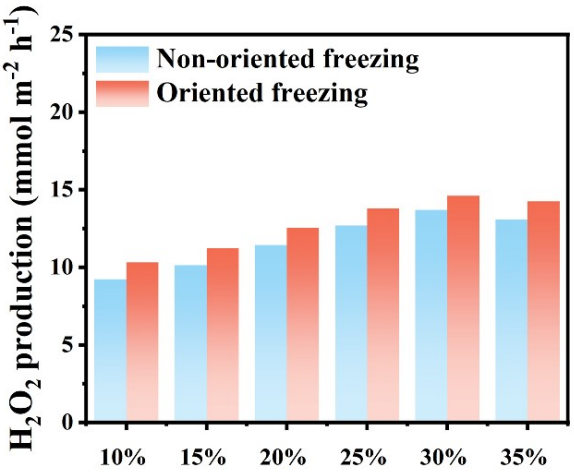

Figure S13. Comparison of H_2O_2 generation rates between oriented and non-oriented aerogels at different PtTt doping levels.

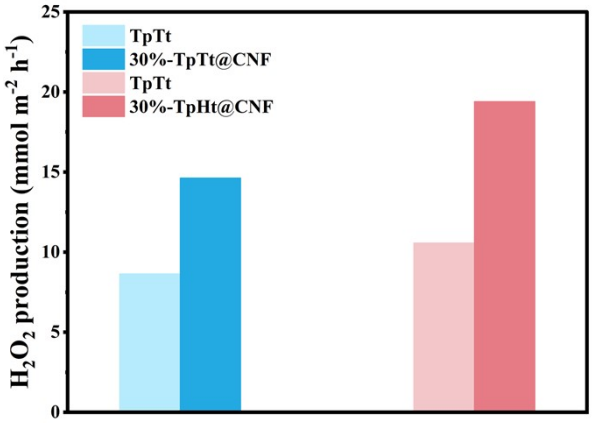

Figure S14. Comparison of photocatalytic H_2O_2 production rates between pristine COFs and their corresponding aerogel samples under identical conditions.

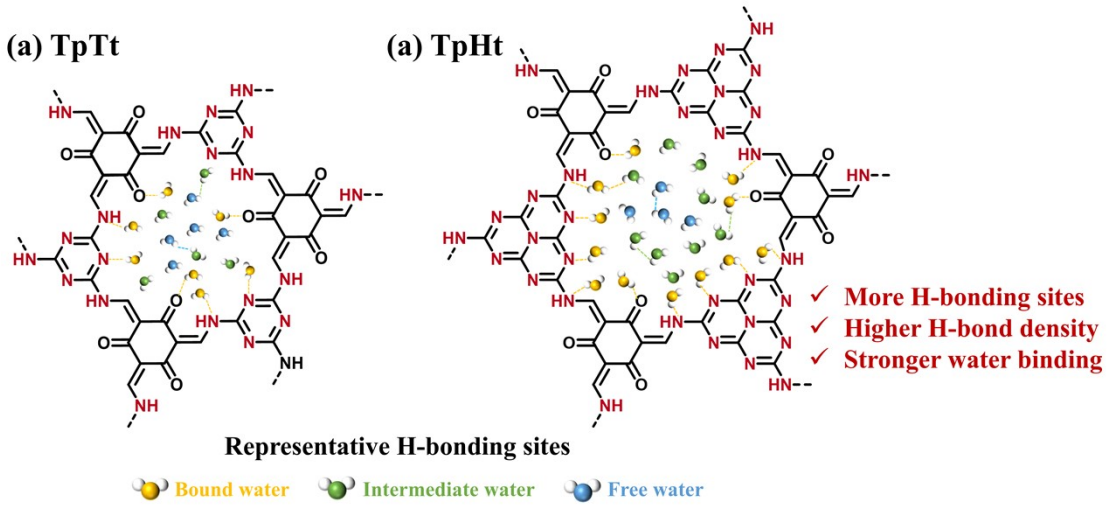

Figure S15. Representative sites in the (a) TpTt and (b) TpHt skeletons regulate the water state by modulating the hydrogen-bonding network.

References

1. C. Shao, Q. He, M. Zhang, L. Jia, Y. Ji, Y. Hu, Y. Li, W. Huang and Y. Li, Chin. J. Catal., 2023, **46**, 28–35.
2. X. Zhong, Q. Ling, Z. Ren and B. Hu, Appl. Catal. B Environ., 2023, **326**, 122398.
3. C. Tang, P. Brodie, Y. Li, N. J. Grishkewich, M. Brunsting and K. C. Tam, Chem. Eng. J., 2020, **392**, 124821.
4. J. Chang, T. Zhang, S. Qiu, N. Huang, D. Pang, H. Li, T. Masese, H. Zhang, Z. Li and Z.-D. Huang, Small, 2023, **19**, 2301579.
5. Y. Zhang, Q. Cao, A. Meng, X. Wu, Y. Xiao, C. Su and Q. Zhang, Adv. Mater., 2023, **35**, 2306831.
6. F. Li, X. Yue, Y. Liao, L. Qiao, K. Lv and Q. Xiang, Nat. Commun., 2023, **14**, 3901.
7. C. Wang, T.-Y. Qiu, Y.-N. Zhao, Z.-L. Lang, Y.-G. Li, Z.-M. Su and H.-Q. Tan, Adv. Energy Mater., 2023, **13**, 2301634.
8. M. Inagaki, T. Tsumura, T. Kinumoto and M. Toyoda, Carbon, 2019, **141**, 580–607.